Clinical Applications of Magnetic Resonance Spectroscopy in Brain Tumors

From Diagnosis to Treatment

Brent D. Weinberg, MD, PhD[a,*], Manohar Kuruva, MD[a], Hyunsuk Shim, PhD[b], Mark E. Mullins, MD, PhD[a]

KEYWORDS

• Brain tumor • Glioblastoma • Magnetic resonance spectroscopy • Pseudoprogression • Radiation necrosis • Tumor progression

KEY POINTS

- Magnetic resonance spectroscopy (MRS) is an advanced MR imaging technique that allows noninvasive evaluation of tissue molecular composition.
- High-grade neoplasms, including brain tumors, have elevation of choline, a marker of cell membrane turnover, with decrease in N-acetyl aspartate, a marker of neuronal integrity.
- The most frequent applications of MRS in brain tumor care are differentiating tumor from other nonneoplastic pathology, estimating tumor grade, and differentiating tumor recurrence from radiation effects.
- Many pathologies overlap in spectroscopic appearance, and MRS is best interpreted in conjunction with other imaging findings and clinical considerations.
- Future developments may make whole-brain spectroscopic imaging a useful tool for prognostication and treatment planning.

INTRODUCTION

Magnetic resonance spectroscopy (MRS) is a technique that combines the ability of nuclear magnetic resonance (NMR) to differentiate molecules with the imaging features of localization unique to MR imaging. This provides a "molecular window" into the component chemistry of a given tissue, allowing for unique insight into physiologic or disease (pathophysiologic) processes. MRS requires no injected contrast agent and no ionizing radiation is involved, which are obvious safety benefits.

There are many applications of MRS to imaging of brain tumors that have been explored, some of which have already reached clinical practice and others that have been confined predominantly to research applications (**Table 1**). In clinical application, MRS can potentially differentiate primary brain tumors from other potential mimics, such as demyelinating disease, lymphoma, or infection. In addition, the "molecular signatures" of high-grade and low-grade tumors often differ, allowing prediction of how aggressive a tumor may be. After treatment, MRS can provide insight into whether treated tissue consists predominantly of radiation necrosis or tumor, a considerable diagnostic dilemma. More research-oriented applications include surveying a tumor to locate the most aggressive area to target for biopsy and

[a] Radiology and Imaging Sciences, Emory University, 1364 Clifton Road Northeast BG20, Atlanta, GA 30322, USA; [b] Radiation Oncology, Emory University, 1365 Clifton Road Northeast, Atlanta, GA 30322, USA
* Corresponding author.
E-mail address: brent.d.weinberg@emory.edu
Twitter: @brentweinberg (B.D.W.)

Radiol Clin N Am 59 (2021) 349–362
https://doi.org/10.1016/j.rcl.2021.01.004

Table 1
Potential uses of magnetic resonance spectroscopy in brain tumor imaging

Clinical Applications	Research Applications
Differentiating tumor from potential mimics	Three-dimensional evaluation of tumor heterogeneity
Metastatic disease	Detection of molecular/genetic features
Demyelinating disease	Isocitrate dehydrogenase mutation
Lymphoma	Treatment planning
Infection	Surgical resection/biopsy
Evaluation of treated tumor to differentiate	Radiation therapy
Recurrent tumor	
Pseudoprogression/radiation necrosis	

radiation therapy by using high-resolution whole brain spectroscopic MR imaging.

MRS has several limitations that have prevented it from reaching its full potential in brain tumor imaging. Despite the theoretic ability to differentiate tissues of different types, there is substantial overlap between the spectroscopic appearances of different diseases. MRS can be time-consuming and highly variable between different imaging locations; moreover, artifacts often limit evaluation.

This work provides an overview of the use of MR spectroscopy in brain tumor imaging, including general imaging principles and technique, key imaged metabolites, the typical appearance of overlapping disease processes, and practical limitations on MRS. The second section discusses ongoing development of new applications likely to have an impact on clinical care in coming years.

IMAGING TECHNIQUE

Early in the development of NMR, it was discovered that nuclei in different molecular environments resonated at slightly different frequencies.[1] In simplest terms, when subjected to an applied magnetic field, molecules precess at a resonant frequency that varies with the surrounding molecular environment. This effect, known as chemical shift, allows nuclei in different chemical environments to be distinguished based on their resonant frequencies. A shielding parameter, defined in parts per million (ppm), describes the relative change compared with a reference compound. The shielding parameter is a constant, whereas the chemical shift measured in Hz increases linearly with field strength. As a result, the resolution of spectroscopy increases with increasing field strength.

Most imaging spectroscopy applications image the hydrogen nucleus (^{1}H) because it is the most prevalent nucleus in tissue. Spectroscopy of other elements is possible,[2] although not used widely in practice. For in vitro proton (^{1}H) spectroscopy, chemical shift values (δ) are reported in ppm relative to a tetramethylsilane (TMS). In vivo, compounds such as TMS are not available, so usually one of the indigenous spectral signals is used as a reference (eg, for the brain, the N-acetyl resonance of N-acetyl aspartate (NAA), set at 2.02 ppm, is often used).

Virtually all MRS studies are performed by collecting time domain data after application of either a 90° pulse, or an echo-type of sequence. The time domain signal is then converted to the frequency domain through Fourier transformation, which allows the viewing of the signal intensity as a function of frequency (ie, in the frequency domain). To accumulate sufficient signal to noise ratio (SNR), the scan can be repeated many (N) times and averaged together to improve SNR, which is proportional to the $\sqrt{N}$. Choosing an appropriate N and scan repetition time (TR) is required to balance image acquisition time and optimize SNR.[3,4] Successful ^{1}H MRS also requires water and lipid suppression techniques, because water and lipids are present at concentrations manyfold higher than target metabolites, which are usually present in the millimolar range. Magnetic field homogeneity and field strengths must be sufficient to allow resolution of the relatively small chemical shift range of protons (~10 ppm). Large and/or membrane-associated molecules are not usually well-seen, although their broad resonances contribute to the baseline of the spectrum.[5]

The information from a brain MR spectrum depends on several factors, such as the field strength, echo time, and type of pulse sequence. On a 1.5 T scanner with long echo times (TE) (eg, 140 or 280 ms), only choline (Cho), creatine (Cr), and NAA are typically observable in healthy adult brain, whereas compounds such as lactate, alanine, or others may be detectable if their concentrations are elevated above normal levels due to abnormal metabolic processes.[6–8] At short TE

($\leq$ 35 ms), additional compounds, including glutamate, glutamine, myo-inositol, lipids, and other macromolecules may become detectable.

Spatial localization allows signals to be recorded from well-defined structures or lesions within the brain.[9–12] In the 1980s, a wide range of spatial localization techniques were developed for in vivo spectroscopy[13]; however, many were either difficult to implement, involved too many radiofrequency pulses, or were inefficient. Out of this plethora of sequences, 2 emerged as simple and robust enough for wider use, each based on 3 slice-selective pulses applied in orthogonal directions. The STEAM sequence (Stimulated Echo Acquisition Mode)[14–17] uses three 90° pulses and detects the resulting stimulated echo from the volume intersected by all 3 pulses, whereas the PRESS sequence (Point REsolved Spectroscopy Sequence)[18,19] uses one 90° pulse and two 180° pulses to detect a spin echo from the localized volume. The sequence is designed so that signals from other regions outside the desired voxel are eliminated (usually by using crusher gradients).[14,20] Typical voxel sizes for brain ^{1}H MRS are approximately 8 cm.[3] Multivoxel (2-dimensional [2D], or 3-dimensional [3D]) PRESS magnetic resonance spectroscopic imaging (MRSI) sequences are available on commercial MR scanners from most scanner vendors and are the most commonly applied MRS technique.[21]

METABOLITES

The most described metabolites in brain tumor spectroscopy are choline, NAA, creatine, lipids, myo-inositol, and lactate (summarized in **Table 2**). A representative normal spectrum from the cerebral hemisphere is shown in **Fig. 1**. The area under each curve represents the number of spins identified; however, this result is only quantitative if an external reference (of known concentration) is used. As such, the areas under the curve are usually evaluated in a relative fashion. Some systems automatically produce relative area under the curve numbers. In the absence of these numbers, peak height is often used as a surrogate marker. Although alterations in the concentrations of each of these metabolites can be seen with various pathologies, a combination of the relative changes of these various metabolites in conjunction with other imaging features can be useful in distinguishing primary brain tumors from metastases, grading gliomas, and distinguishing recurrence from radiation necrosis. Sometimes, ratios of metabolites (such as Cho/Cr, or Cho/NAA) can be used to increase the sensitivity of a particular measure. In practice, this is one of the most commonly used approaches.

Cho (3.2 ppm) is a precursor of acetylcholine, a component of cell membranes. Elevated Cho is a marker of increased cell turnover, which can be seen with tumors and other proliferative processes. In combination with other imaging features, elevated Cho can identify high cellular turnover pathologies like gliomas and lymphoma compared with other pathologies with lower cellularity, such as radiation necrosis or infarction.[22,23]

NAA (2.0 ppm) is synthesized from acetylation of the amino acid aspartate in the neuronal mitochondria and is a marker of neuronal viability. Reduction of NAA is seen in many pathologies, such as glioma and radiation necrosis, which involve destruction or replacement of neurons. Lymphoma or metastases tend to show low or absent NAA levels due to lack of neurons in the tumor component.[24]

Cr (3.0 ppm) has a role in storage and transfer of energy in neurons that have high metabolism. Cr is relatively maintained across a number of disease processes and serves as an internal control which can be used for ratio calculations, such as Cho/Cr.

Lactate (Lac, 1.3 ppm) is a marker of anerobic metabolism and is not seen in normal adult brain spectra due to exclusive aerobic metabolism in brain. Lactate is visualized in necrotic tissues with anerobic metabolism which include abscesses and high-grade tumors.[25,26] Lactate overlaps with lipids at short TE, shows inversion at intermediate TE, and has a characteristic double peak at longer TE.[27]

Lipids (Lip, 1.3 ppm) are components of cell membrane and are increased in diseases with high cell turnover rates such as high-grade gliomas (HGGs). However this is not a specific feature and can be see with other pathologies with high cell turnover/destruction such as abscesses, infarction, and metastases.[28]

Myo-Inositol (MI, 3.5 ppm) is a precursor of phosphatidylinositol (a phospholipid) and of phosphatidylinositol 4,5-bisphosphate. Elevations of MI are seen in low-grade gliomas; in contradistinction, reduction seen in World Health Organization grade IV gliomas and can be a useful marker in grading gliomas.[29] Elevation of MI can also be seen with other pathologies like dementia of Alzheimer type and progressive multifocal leukoencephalopathy.

2-Hydroxyglutarate (2-HG, 2.25 ppm) is an oncometabolite of increasing interest in recent times. Tumors with isocitrate dehydrogenase (IDH-1) mutations accumulate higher levels of 2-HG, and as a result detection of 2-HG can be used with reasonable accuracy for noninvasive detection of IDH-1 mutant gliomas.[30]

Table 2
Frequently encountered metabolites and their characteristics and clinical role in evaluating brain tumors

Metabolite	ppm	Elevated in	Decreased in	Clinical Significance in Brain Tumor Imaging
Choline	3.2 ppm	Neoplasms Inflammation Gliosis	Necrosis	Grading gliomas Distinguishing glioblastomas for metastases Radiation planning in gliomas Differentiating tumor progression vs pseudoprogression/ Radionecrosis
N-acetyl aspartate	2.0 ppm		Gliomas and more so in high-grade gliomas Radiation necrosis Metastases Lymphoma	Grading of gliomas Distinguishing gliomas from metastases
Creatine	3.0 ppm		High-grade gliomas Necrosis	Grading of gliomas Distinguishing metastases from glioblastoma
Lactate	1.3 ppm	Glioblastoma Abscesses	Not present in normal spectra	Grading of gliomas
Lipids	1.3 ppm with inversion at intermediate echo time	Glioblastoma Abscess Lymphoma Metastases		Grading of gliomas
Myo-Inositol	3.5 ppm	Low-grade gliomas Progressive multifocal encephalopathy	High-grade gliomas	Grading of gliomas
2-Hydroxyglutarate	2.5 ppm	Isocitrate dehydrogenase (IDH)-1 positive tumors		Detection of IDH-1 positive tumors

Other metabolites have been described in the research setting, including metabolites of other nuclei.[31,32] However, these have demonstrated little clinical importance.

CLINICAL RELEVANCE: DIAGNOSIS

Years ago, brain tumor workups commonly involved a 2-step process including an initial needle biopsy followed by a more definitive surgical resection. The transition to what is usually a single (initial) surgery has been ushered along by developments in neuroimaging, including advanced techniques. MRS is one of those techniques and, along with other methods, this constellation of imaging tools essentially serves as a sort of "virtual biopsy." In complex cases, such an approach can be used to differentiate gliomas from other diagnoses such as metastases, lymphoma, demyelination, edema, necrosis, and infection. Unfortunately, the spectroscopic profile of HGGs overlaps that of other brain tumors and even non-neoplastic diagnoses on many occasions. It is important to use advanced neuroimaging such as MRS in the context of conventional imaging, including MR imaging.

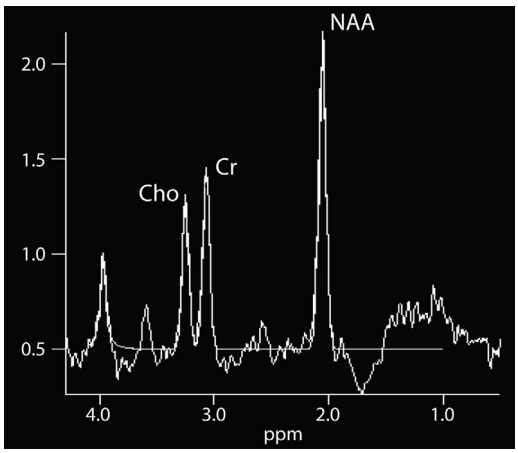

Fig. 1. MRS spectrum from an area of normal brain. Cho, Cr, and NAA are the dominant peaks, with NAA higher than both Cho and Cr.

Brain metastases, particularly when solitary, can have considerable overlap with the appearance of primary brain tumors on MR imaging. Both are characterized by enhancing masses with surrounding T2/fluid attenuated inversion recovery (FLAIR) hyperintense edema. Both metastases and gliomas are known to have elevated Cho and decreased NAA compared with adjacent normal white matter. However, lipids and macromolecules are higher in metastases than glioblastoma.[33] Evaluating spectroscopic results for the edema next to an enhancing mass may help with diagnosis, as the edema in gliomas more often contains infiltrating tumor cells and as a result has higher Cho/NAA and Cho/Cr.[24,33–35] As an example of this approach, please see **Fig. 2**. Placement of voxels within the enhancing abnormality is suggestive of a high-grade tumor (either glioma or metastasis), but elevated Cho in the nonenhancing abnormality is more consistent with a high-grade tumor.

Primary central nervous system lymphoma (PCNSL) also can mimic primary brain tumors in many cases; however, there remains some hope for the utility of MRS in these instances. For example, Nagashima and colleagues[36] recently reported that MI was significantly increased in HGGs compared with PCNSL. In addition to absolute value measurements, peak ratios have also been used to assist with differentiation. High-grade tumors such as lymphoma and HGG have higher elevation of Cho/NAA compared with nonneoplastic diagnoses, such as demyelination.[37] Although both lymphoma and HGG have Cho/NAA elevation, lymphoma is reported to have lower Cho/NAA than primary brain tumors.[38] **Fig. 3** shows an example of a patient with periventricular abnormality on brain MR imaging that is, most consistent with primary central nervous lymphoma on conventional imaging. MR spectroscopy in this setting was consistent with high-grade tumor (**Fig. 3**). Spectroscopy does rule out other

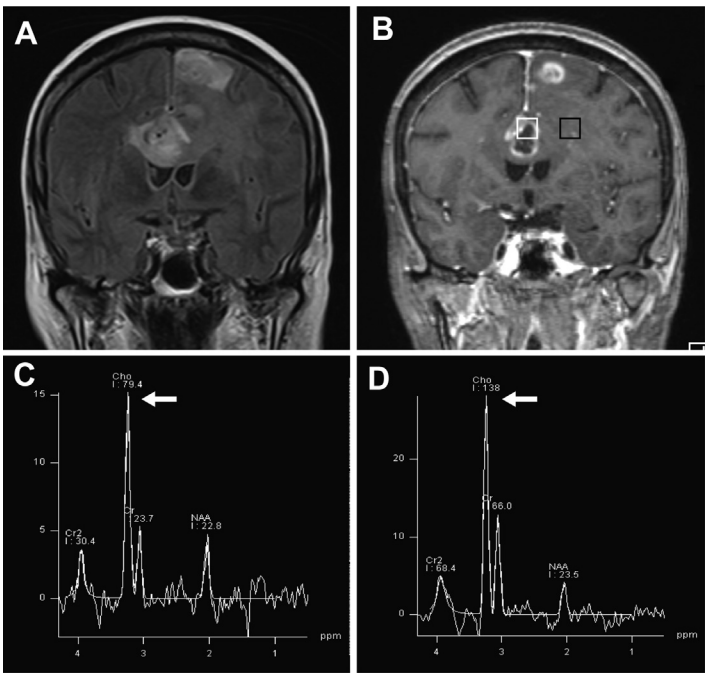

Fig. 2. Glioblastoma. An 86 year-old woman with new neurologic symptoms. Coronal FLAIR (*A*) and contrast-enhanced T1-weighted images (*B*) demonstrate a mass in the corpus callosum and left superior frontal gyrus with multiple areas of enhancement. Spectroscopy (TE 144 ms) from the corpus callosum (*C*, region of *white box* in *B*) shows markedly elevated Cho (*white arrow*) and relatively low NAA. Spectroscopy from the area of nonenhancing tumor in the left centrum semiovale (*D*, *black box* in *B*) shows similar findings in the nonenhancing areas, confirming infiltrative tumor.

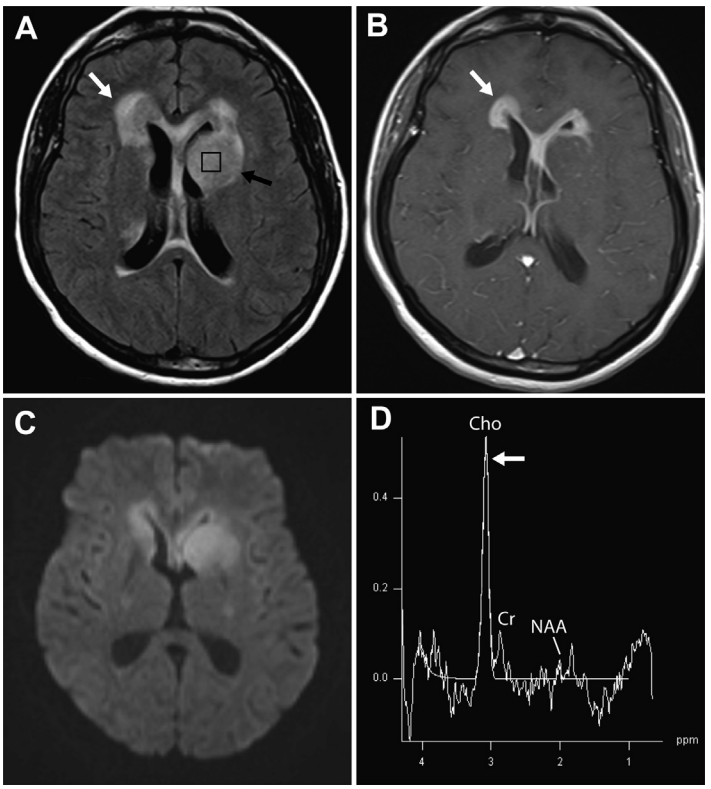

Fig. 3. Lymphoma. A 40 year-old woman with human immunodeficiency virus presented with altered mental status. FLAIR (*A*) though the basal ganglia showed masslike FLAIR hyperintensity and expansion of the left caudate (*black arrow*) with multiple periventricular masses that enhance on postcontrast T1-weighted images (*B*, *white arrows*). DWI (*C*) demonstrates associated hyperintensity. Spectroscopy (TE 140 ms) (*D*) from the caudate (*black box, A*) shows markedly elevated Cho (*white arrow*) with very low Cr and NAA.

possibilities such as infection in this case, although this appearance could easily be confused with glioblastoma, highlighting the importance of interpreting MRS alongside conventional imaging. For further review of intracranial lymphoma including MRS see an article by Brandao and Castillo.[39]

Tumefactive demyelinating lesions (TDLs) have an overlapping appearance with primary brain tumors. Results have been conflicting regarding the value of MRS in these cases. Ikeguchi and colleagues[40] found that a Cho/NAA ratio greater than 1.72 favors HGG over TDL. These results contrast with those of Saindane and colleagues[41] who found no difference Cho/Cr ratios in contrast-enhancing, central, or perilesional areas of TDLs and gliomas. TDL are most associated with loss of normal neuronal peaks including Cr and NAA. **Fig. 4** shows an example of tumefactive demyelination that has a typical appearance on conventional imaging. The MR spectroscopic results are most notable for the presence of prominent lactate and absence of peak ratios suggestive of high-grade tumor (**Fig. 4**). In our experience, prominent lactate is rarely associated with untreated brain tumors.

Another type of brain mass that can occasionally be misinterpreted as primary brain tumor is pyogenic brain abscess. The conventional imaging, especially diffusion-weighted imaging (DWI) and apparent diffusion coefficient evaluation of the central nonenhancing material is traditionally quite helpful. As one might imagine, identification of lactate commonly overlaps both entities.[42] The classic MRS description of abscess includes presence of amino acid peaks such as valine, alanine, leucine, acetate, and succinate.[42] However, Pal and colleagues[43] found that amino acids, although found in 80% of abscesses, had a sensitivity and specificity of 0.72 and 0.30, respectively. The clinical utility of numbers like these is unclear at best.

To summarize, a Venn diagram of MRS for astrocytoma/glioma, lymphoma, TDL, and brain abscess would not have distinct circles. An individual patient may have an MRS pattern that suggests one of these diagnoses, but this result is best interpreted in the setting of the conventional MR imaging results and the clinical presentation. A combination of peak presence (especially combinations), peak height, area under the (peak) curve, and peak ratio may be helpful, whereas individual values are challenging to interpret. Future work using MRS as a multiparametric biomarker, including incorporation of machine learning techniques, may increase its ability to differentiate these diagnoses and predict patient prognosis.[34] In reviewing the literature, it is clear that the consensus is that there is no consensus.

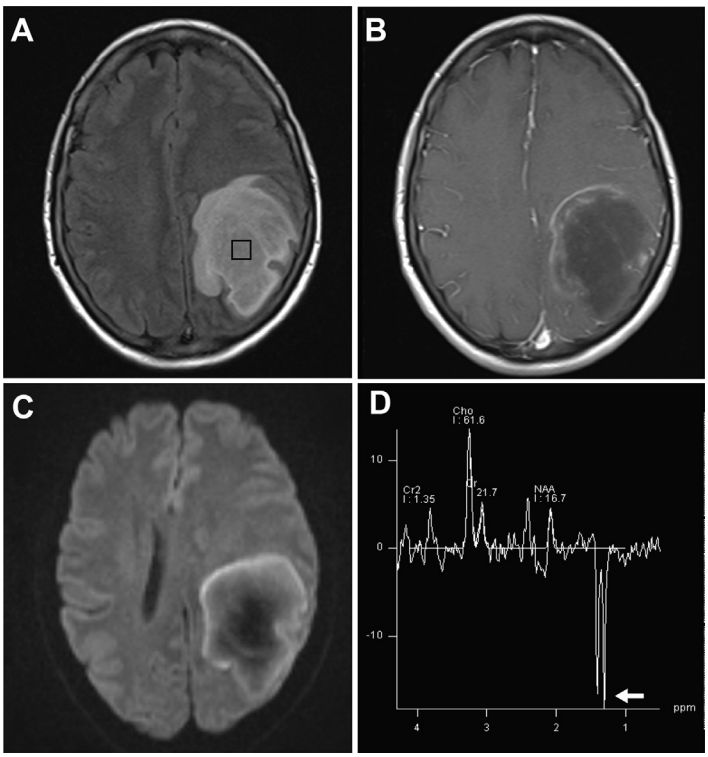

Fig. 4. Tumefactive demyelination. A 50-year-old woman with right-sided weakness. FLAIR (*A*) images show an expansile, FLAIR hyperintense mass in the left parietal lobe with a peripheral incomplete rim of enhancement on T1-weighted imaging (*B*). DWI (*C*) similarly shows a peripheral rim of abnormally hyperintense DWI. Spectroscopy (TE 135 ms) (*D*) from the central portion of the lesion (*black box*, *A*) shows elevated Cho, near complete loss of NAA, and a characteristic inverted doublet lactate peak at 1.3 ppm.

CLINICAL RELEVANCE: TUMOR GRADING

MRS has a clinical role in grading gliomas. In conjunction with other imaging features like hemorrhage, necrosis, and enhancement it can be useful to support a diagnosis of HGG versus low-grade glioma. Typical abnormal spectroscopic features of low-grade gliomas include modest Cho elevation, NAA reduction, and Cho/Cr ratio elevation (**Fig. 5**). MI and MI/Cr ratio can also be elevated. Low-grade gliomas typically lack Lac and Lip peaks. In some cases, low-grade gliomas may have only mild changes in Cho or NAA with some changes in MI. Therefore, it should be noted that short TE spectroscopy with more detectable metabolites is helpful in low-grade gliomas.

HGGs tend to have more dramatic MRS changes compared with low-grade tumors. Typical MRS features of grade III and IV gliomas include increased Cho and decreased Cr, NAA, and MI (**Fig. 2**). NAA is seen in higher concentrations in low-grade gliomas relative to HGGs and can be used as a marker of prognosis and grading gliomas.[44] Reductions in Cr can be seen and in combination with increased Cho results in higher Cho/Cr ratios in HGGs compared with low-grade gliomas.[44] There can be variations in spectroscopy abnormalities in glioblastoma depending on the area sampled, and sampling of necrotic regions may show only lipid and lactate peaks with reduced/absent Cho peak. Presence of lactate and lipid peaks suggests a grade IV tumor and is not commonly seen with grade III gliomas.

As there is considerable overlap in spectroscopy patterns of low-grade versus HGGs, semiquantitative analysis using ratios of various metabolites is used to better predict the grade. Commonly used ratios are Cho/Cr, Cho/NAA, and NAA/Cr. Typical pattern in HGGs is elevated Cho/Cr, Cho/NAA ratios and reduced NAA/Cr ratio. Cho/Cr is the most commonly used in clinical practice and in research studies. Wang and colleagues,[45] in a large meta-analysis, looked at 30 articles comprising 1228 patients and analyzed utility of various metabolite ratios in predicting grade of gliomas and distinguishing low-grade gliomas from HGGs. Quantitative synthesis of studies showed that the pooled sensitivity/specificity of Cho/Cr, Cho/NAA and NAA/Cr ratios was 0.75/0.60, 0.80/0.76 and 0.71/0.70, respectively. The area under the curve values for these metabolites were 0.83, 0.87, and 0.78, respectively. In this analysis, all 3 ratios had comparable performance and Cho/NAA ratio showed the highest accuracy. However, it should be noted that there was wide variation in the ratio cutoffs used in these studies.

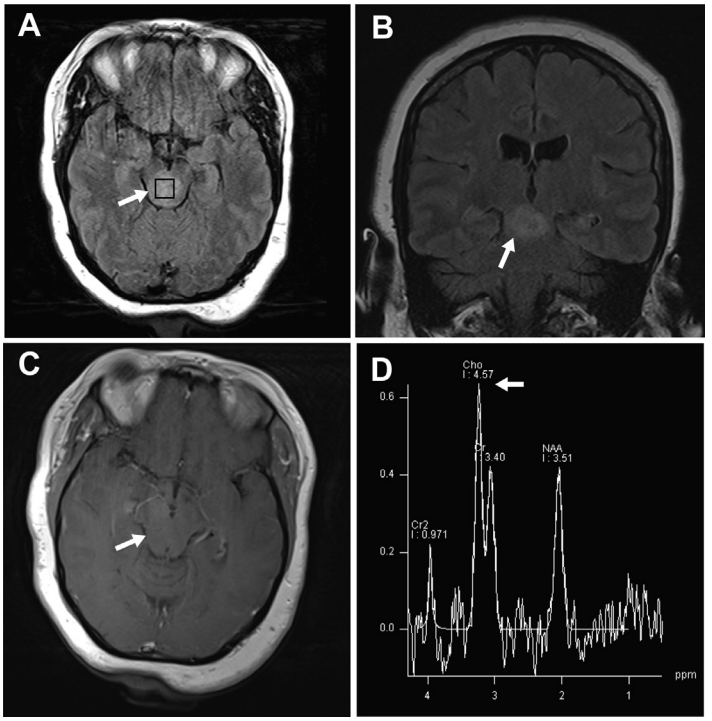

Fig. 5. Low-grade glioma. A 34-year-old woman with neurofibromatosis type 1. Axial (*A*) and coronal (*B*) FLAIR images show an expansile mass within the midbrain with no enhancement on postcontrast T1-weighted images (*C*) (*arrows*). Spectroscopy (TE 135 ms) (*D*) within the midbrain shows modest elevation of Cho (*arrow*) and depression of NAA. Spectroscopy is particularly important in this difficult to biopsy location.

CLINICAL RELEVANCE: FOLLOW-UP

MRS can be useful in the longitudinal follow-up of patients with brain tumor, particularly for troubleshooting cases in which there may be significant overlap between tumor progression and radiation effects. Worsening in both post–contrast enhancement on T1-weighted imaging and surrounding FLAIR hyperintense edema can both occur because of radiation injury to the tumor and surrounding normal tissue.[46] Pseudoprogression is the phenomenon of acute imaging worsening in the early phase after radiation, usually within the first 3 to 6 months after completing chemoradiation.[47] Pseudoprogression can occur in as many as 20% to 30% of primary brain tumors and is more common in patients with O6-methylguanine–DNA methyltransferase methylation.[48] Furthermore, pseudoprogression is associated with improved patient outcomes. It is important to differentiate pseudoprogression from true tumor progression, as tumor progression in this early period would indicate a failure of initial therapy, which would necessitate a change in therapy, often taking a patient off the well-tolerated and often effective temozolomide to begin another therapy such as lomustine. Interpretation guidelines such as the Response Assessment in Neuro-Oncology advise conservative interpretation of cases in the first 3 months after completing radiation, assuming imaging worsening is pseudoprogression as long as they occur in the radiation treatment field.[49] Pseudoprogression is usually self-limited,[47] and when imaging does not improve on subsequent follow-up, interpretation is more nuanced and determining if worsening represents tumor progression is more challenging. Radiation necrosis can also occur in a delayed fashion any time from months to years after completing radiation therapy. It can have progressive worsening of enhancement, edema, and mass effect along with worsening patient symptoms. Later, radiation necrosis poses a considerable diagnostic dilemma because of its highly variable timing.

Advanced imaging, including MRS, can be a useful tool in differentiating treatment effects from tumor progression, and the imaging appearance of pseudoprogression and delayed radiation necrosis are similar. Radiation results in decreased NAA, Cho, and Cr compared with patients with tumor recurrence.[46] Using ratios including Cho/Cr can further improve performance of spectroscopy, with higher Cho/Cr in cases of tumor progression. In a meta-analysis of 477 lesions, MRS had moderate performance in differentiating radiation necrosis from glioma recurrence, with Cho/Cr ratio having a sensitivity, specificity, and areas under the curve of 0.83, 0.83, and 0.91, respectively.[50] Compared with progressive tumor, radiation necrosis is also more likely to show elevation in Lip and Lac (**Fig. 6**).[51]

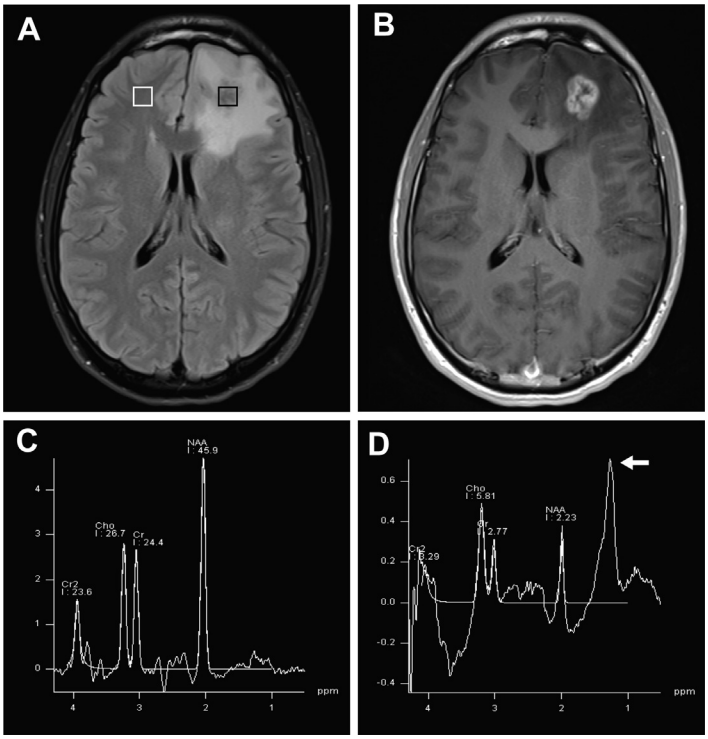

Fig. 6. Radiation necrosis. A 21-year-old with Ewing sarcoma metastasis to the left frontal lobe previously treated with radiation. Expansile mass in the left frontal lobe with surrounding abnormal FLAIR (*A*) and central enhancement on postcontrast T1 (*B*). Spectroscopy (TE 135 ms) of the contralateral normal white matter (*C*, from *white box* in *A*) shows relatively normal spectrum. Spectroscopy of the abnormal region (*D*, from *black box* in *A*) shows decrease in height of all peaks, particularly NAA, with a lipid/lactate peak at 1.3 ppm (*white arrow*).

MRS has performed similar or better than other advanced techniques for evaluating potential radiation necrosis.[52] MR perfusion has shown promise in evaluating necrosis, with hyperperfusion associated with tumor recurrence.[46] PET with both fludeoxyglucose F 18 and ^{11}C-methionine, an amino acid tracer, have had intermediate results. Quantitative diffusion imaging has also been relatively promising (sensitivity 75%, specificity 88.9%), with radiation necrosis having greater reduction in central apparent diffusion coefficient values.[53] Combined approaches using MRS in conjunction with other advanced imaging may have the best performance.

LIMITATIONS

Use of MRS in evaluation and follow-up of brain tumors has several significant limitations. The primary limitation is the considerable overlap between the spectroscopic appearance of different pathology. Each pathology has characteristic features that may occur most commonly, but typical diagnostic accuracy may range from 60% to 80%. However, because of overlapping appearance, many times short-term follow-up imaging (4–6 weeks) or surgical biopsy are required to confirm a diagnosis. The lack of definitive imaging findings has been the primary reason MRS is not used more frequently. Other technical limitations also confound implementation of MRS. Imaging sites and scanners vary widely in their implementation, and there is little widespread standardization of imaging techniques. Artifacts and noise are common and further limit interpretation. Susceptibility from adjacent bone or air limit signal from portions of the brain near the skull base and calvarium. Averaging of all signal within relatively large voxels limits evaluation of small lesions, and incomplete water and lipid suppression can completely obscure the diagnostic signal. Imaging can also be time-consuming and require technologist or radiologist intervention. All these limitations are the subject of ongoing research and development.

FUTURE DIRECTIONS

Research is currently under way to improve current technology and develop and new applications to increase the clinical usefulness of MRS in brain tumor diagnosis and treatment. Sequence development is geared toward improving resolution, brain coverage, and speed while decreasing artifacts. Conventional Cartesian 2D or 3D phase-encoding approaches can give excellent quality data, but they rapidly become too time-consuming with increasing spatial resolution and brain coverage. A

number of methods to accelerate MRS have been described, include parallel imaging and compressed sensing.[54–56] Alternative strategies are required to increase acquisition speed by an order of magnitude or more; echo-planar spectroscopic imaging (EPSI) is one of the oldest but also one of the fastest acceleration methods for MRS.[57–60] In EPSI, k-space is traversed in a rectilinear manner by the oscillating read gradient that is, applied simultaneously with spectral data acquisition. For a 3D acquisition, the other 2 dimensions are encoded using conventional (or elliptical) phase-encoding. Scan times can be reduced even further through undersampling approaches such as SENSE or GRAPPA in these dimensions.[61–63] When combined with advanced water and lipid suppression techniques, EPSI can be used to obtain high-resolution whole-brain spectroscopic maps with scan times ranging from 10 to 18 minutes.[58,64,65] Smaller voxel sizes result in decreased artifact from surrounding structures and less partial volume artifact. Whole-brain coverage further allows novel applications such as biopsy[66] and treatment planning. These applications are not limited by overlap between different pathology, as the disease of often already known and MRS is being used to define the involved region.

Using MRS to choose optimal biopsy sites is made possible by whole-brain spectroscopic imaging. Brain tumors are highly infiltrative, and diagnosis of grade II and III gliomas can be particularly challenging because they are heterogeneous tumors that can lack well-defined enhancement.[67] Biopsy is taken from areas of hyperintensity on T2/FLAIR images, but this does not account for areas of tumor heterogeneity and can result in undersampling of high-grade or anaplastic areas.[68–70] Whole-brain EPSI can be a useful adjunct to conventional imaging to guide biopsy target selection, with Cho or Cho/NAA maps overlaid on anatomic images and uploaded to surgical guidance software to choose a biopsy site (**Fig. 7**) (Zhong et al., manuscript in preparation). Greater metabolite abnormalities are associated with more proliferative areas, and sampling these regions maximizes the chance of sampling high-grade areas.[44,71]

Advanced treatment planning is also a potential application of whole-brain MRS.[72–75] In grade IV tumors, high-dose radiation is targeted to the resection cavity and areas of residual contrast enhancement that may underrepresent areas of infiltrative tumor.[71] Recurrence can then occur in

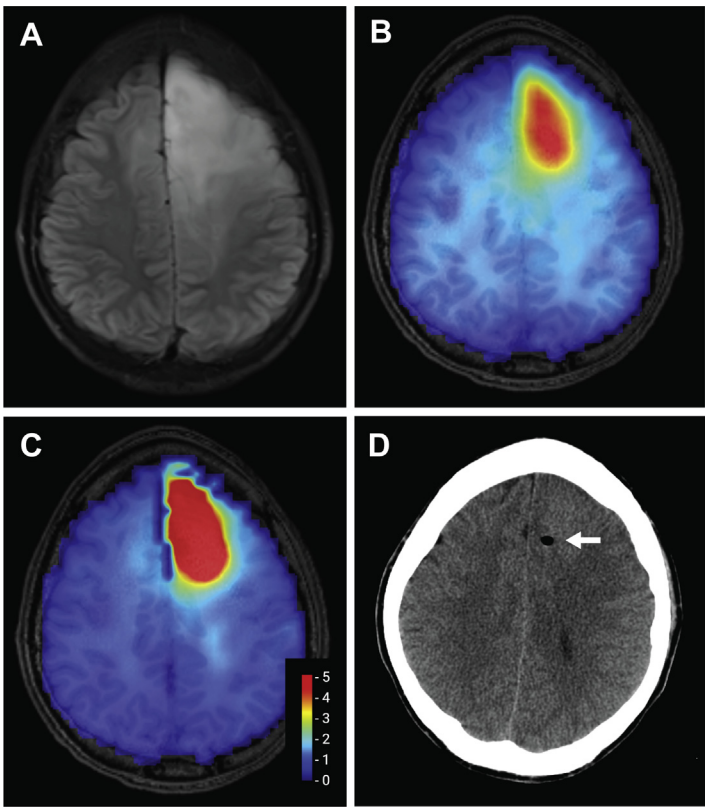

Fig. 7. Grade 3 astrocytoma. A 31-year-old man with a left frontal expansile, nonenhancing mass seen on FLAIR (*A*). T1-weighted images overlaid with 3D Cho map (*B*) and Cho/NAA ratio (*C*), showing areas of greatest metabolic abnormality. Scale in (*C*) shows the ratio between Cho/NAA and normal white matter. Stereotactic biopsy was targeted to a region with maximal metabolic abnormality, as seen on post-biopsy CT (*D*).

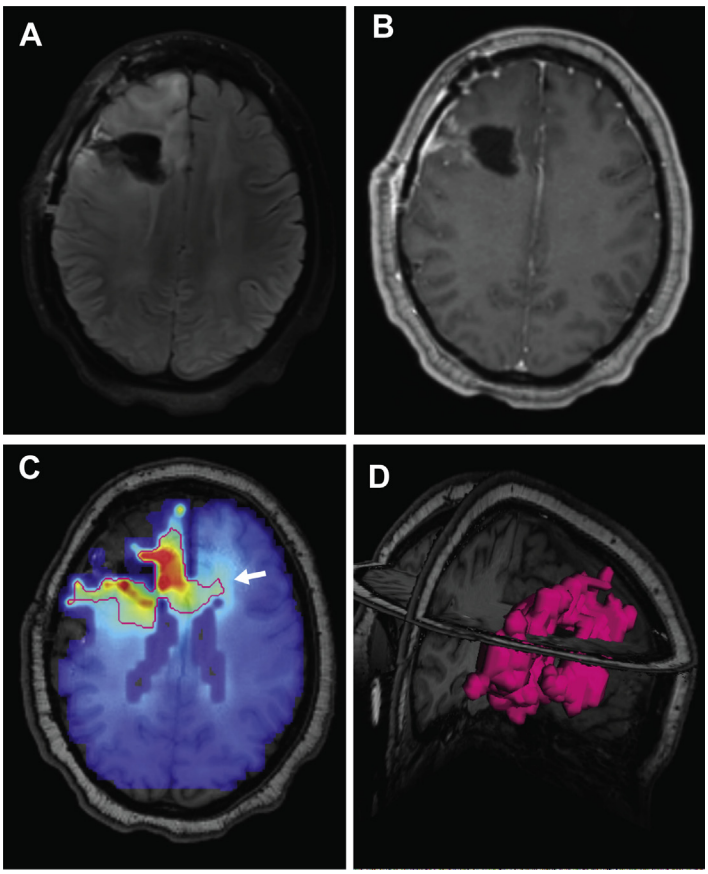

Fig. 8. Glioblastoma. Right frontal glioblastoma, status post resection. FLAIR abnormality surrounds the cavity in the right middle and superior frontal gyri (*A*). A small amount of nodular enhancement is present around the cavity on postcontrast T1-weighted imaging (*B*). T1-weighted images overlaid with 3D Cho/NAA ratio (*C*) show tumor extending beyond the area of abnormal enhancement and FLAIR (*white arrow*). The red line outlines the area with a Cho/NAA ratio 2 times normal white matter, a threshold associated with 30% tumor in previous biopsy studies. Three-dimensional rendering of area of MRS abnormality surrounding the resection cavity (*D*).

surrounding areas undertreated by existing radiation plans. An improved strategy might be to treat areas of greater spectroscopic abnormality, such as those with elevated Cho/NAA ratio, with high-dose radiation to the area meeting a threshold difference from normal white matter (**Fig. 8**). A multisite clinical trial recently completed patient enrollment to test this approach (NCT03137888) and is currently in the follow-up period.[76]

SUMMARY

MRS is an advanced technique that allows for molecular evaluation of tissue composition without contrast or radiation. It has a valuable role in the diagnosis, treatment, and subsequent evaluation of patients with brain tumor, particularly as a troubleshooting tool when conventional imaging findings of 2 diagnoses overlap. Unfortunately, overlap between spectroscopy findings and technical considerations limit its accuracy, MRS is most useful when interpreted in conjunction with MR imaging findings and other advanced techniques. Future developments promise faster and more accurate MRS, which can be applied to novel applications such as biopsy and treatment planning.

CLINICS CARE POINTS

- Magnetic resonance spectroscopy (MRS) is a useful troubleshooting tool which can be used in advanced imaging of brain tumors to differentiate tumor from other pathology and estimate tumor grade.
- Tumors are characterized by high cell turnover, resulting in elevated choline (Cho), and replacement of normal neurons, resulting in decreased N-acetyl aspartate (NAA).
- Greater elevation in choline (Cho) is associated with more aggressive tumors and other neoplastic pathologies such as lymphoma, while non neoplastic pathologies often manifest other peaks including lactate/lipids and myo-inositol.
- Because of considerable overlap between spectroscopic findings between a variety of pathology, spectroscopy results should be interpreted in the context of other imaging findings and clinical presentation.

DISCLOSURE

Funding for this project includes NIH/NCI R01 CA214557 and NIH/NIBIB U01 EB028145 (PI: Shim) and RSNA Scholar grant (PI: Weinberg).

REFERENCES

1. Proctor WG, Yu FC. The dependence of a nuclear magnetic resonance frequency. Phys Rev 1950;77:717.
2. Julia-Sape M, Candiota AP, Arus C. Cancer metabolism in a snapshot: MRS(I). NMR Biomed 2019; 32(10):e4054.
3. Ernst RR, Anderson WA. Application of Fourier transform spectroscopy to magnetic resonance. Rev Sci Instrum 1966;37:93–102.
4. Ernst RR, Bodenhausen G, Wokaun A. Principles of nuclear magnetic resonance in one and two dimensions, vol. 1. New York: Oxford University Press; 1990.
5. Behar KL, Ogino T. Characterization of macromolecule resonances in the 1H NMR spectrum of rat brain. Magn Reson Med 1993;30(1):38–44.
6. Barker PB, Gillard JH, van Zijl PC, et al. Acute stroke: evaluation with serial proton MR spectroscopic imaging. Radiology 1994;192(3):723–32.
7. Lin DD, Crawford TO, Barker PB. Proton MR spectroscopy in the diagnostic evaluation of suspected mitochondrial disease. AJNR Am J Neuroradiol 2003;24(1):33–41.
8. Remy C, Grand S, Lai ES, et al. 1H MRS of human brain abscesses in vivo and in vitro. Magn Reson Med 1995;34(4):508–14.
9. Luyten PR, den Hollander JA. Observation of metabolites in the human brain by MR spectroscopy. Radiology 1986;161(3):795–8.
10. Hanstock CC, Rothman DL, Prichard JW, et al. Spatially localized 1H NMR spectra of metabolites in the human brain. Proc Natl Acad Sci U S A 1988;85(6):1821–5.
11. Bottomley PA, Edelstein WA, Foster TH, et al. In vivo solvent-suppressed localized hydrogen nuclear magnetic resonance spectroscopy: a window to metabolism? Proc Natl Acad Sci U S A 1985;82(7): 2148–52.
12. Bax A, Freeman R. Enhanced NMR resolution by restricting the effective sample volume. J Magn Reson 1980;37:177–81.
13. Aue WP. Localization Methods for in vivo NMR spectroscopy. Rev Magn Reson Med 1986;1:21–72.
14. Frahm J. Localized Proton Spectroscopy using stimulated echoes. J Magn Reson 1987;72(3):502–8.
15. Frahm J, Bruhn H, Gyngell ML, et al. Localized high-resolution proton NMR spectroscopy using stimulated echoes: initial applications to human brain in vivo. Magn Reson Med 1989;9(1):79–93.
16. Granot J. Selected Volume Excitation Using Stimulated Echoes (VEST). Applications to spatially localized spectroscopy and imaging. J Magn Reson 1986;70(3):488–92.
17. Kimmich R, Hoepfel D. Volume-selective multipulse spin-echo spectroscopy. J Magn Reson 1987; 72(2):379–84.
18. Bottomley PA, Inventor; General Electric Company, assignee. Selective volume method for performing localized NMR spectroscopy. US patent 4480228. October 30th 1984, 1984.
19. Ordidge RJ, Gordon RE, Inventors; Oxford Research Systems Limited, assignee. Methods and apparatus of obtaining NMR spectra. US patent 45310941983.
20. van Zijl PC, Moonen CT, Alger JR, et al. High field localized proton spectroscopy in small volumes: greatly improved localization and shimming using shielded strong gradients. Magn Reson Med 1989; 10(2):256–65.
21. Nelson SJ. Analysis of volume MRI and MR spectroscopic imaging data for the evaluation of patients with brain tumors. Magn Reson Med 2001;46(2): 228–39.
22. Brandão LA, Castillo M. Adult brain tumors: clinical applications of magnetic resonance spectroscopy. Magn Reson Imaging Clin N Am 2016;24(4): 781–809.
23. Shimizu H, Kumabe T, Shirane R, et al. Correlation between choline level measured by proton MR spectroscopy and Ki-67 labeling index in gliomas. AJNR Am J Neuroradiol 2000;21(4):659–65.
24. Server A, Josefsen R, Kulle B, et al. Proton magnetic resonance spectroscopy in the distinction of high-grade cerebral gliomas from single metastatic brain tumors. Acta Radiol 2010;51(3):316–25.
25. Fan G. Comments and controversies: magnetic resonance spectroscopy and gliomas. Cancer Imaging 2006;6:113–5.
26. Lai PH, Ho JT, Chen WL, et al. Brain abscess and necrotic brain tumor: discrimination with proton MR spectroscopy and diffusion-weighted imaging. AJNR Am J Neuroradiol 2002;23(8):1369–77.
27. Yamasaki F, Takaba J, Ohtaki M, et al. Detection and differentiation of lactate and lipids by single-voxel proton MR spectroscopy. Neurosurg Rev 2005; 28(4):267–77.
28. Brandão LA, Castillo M. Adult brain tumors: clinical applications of magnetic resonance spectroscopy. Neuroimaging Clin N Am 2013;23(3):527–55.
29. Castillo M, Smith JK, Kwock L. Correlation of myo-inositol levels and grading of cerebral astrocytomas. AJNR Am J Neuroradiol 2000;21(9):1645–9.
30. Suh CH, Kim HS, Jung SC, et al. Imaging prediction of isocitrate dehydrogenase (IDH) mutation in patients with glioma: a systemic review and meta-analysis. Eur Radiol 2019;29(2):745–58.

31. Grist JT, Miller JJ, Zaccagna F, et al. Hyperpolarized (13)C MRI: A novel approach for probing cerebral metabolism in health and neurological disease. J Cereb Blood Flow Metab 2020;40(6):1137–47.
32. Wenger KJ, Hattingen E, Franz K, et al. In vivo metabolic profiles as determined by (31)P and short TE (1)H MR-spectroscopy : no difference between patients with IDH wildtype and IDH mutant gliomas. Clin Neuroradiol 2019;29(1):27–36.
33. Pope WB. Brain metastases: neuroimaging. Handb Clin Neurol 2018;149:89–112.
34. Durmo F, Rydelius A, Cuellar Baena S, et al. Multivoxel (1)H-MR spectroscopy biometrics for preoperative differentiation between brain tumors. Tomography 2018;4(4):172–81.
35. Chiang IC, Kuo YT, Lu CY, et al. Distinction between high-grade gliomas and solitary metastases using peritumoral 3-T magnetic resonance spectroscopy, diffusion, and perfusion imagings. Neuroradiology 2004;46(8):619–27.
36. Nagashima H, Sasayama T, Tanaka K, et al. Myo-inositol concentration in MR spectroscopy for differentiating high grade glioma from primary central nervous system lymphoma. J Neurooncol 2018;136(2):317–26.
37. Lu SS, Kim SJ, Kim HS, et al. Utility of proton MR spectroscopy for differentiating typical and atypical primary central nervous system lymphomas from tumefactive demyelinating lesions. AJNR Am J Neuroradiol 2014;35(2):270–7.
38. Vallee A, Guillevin C, Wager M, et al. Added value of spectroscopy to perfusion MRI in the differential diagnostic performance of common malignant brain tumors. AJNR Am J Neuroradiol 2018;39(8):1423–31.
39. Brandao LA, Castillo M. Lymphomas-Part 1. Neuroimaging Clin N Am 2016;26(4):511–36.
40. Ikeguchi R, Shimizu Y, Abe K, et al. Proton magnetic resonance spectroscopy differentiates tumefactive demyelinating lesions from gliomas. Mult Scler Relat Disord 2018;26:77–84.
41. Saindane AM, Cha S, Law M, et al. Proton MR spectroscopy of tumefactive demyelinating lesions. AJNR Am J Neuroradiol 2002;23(8):1378–86.
42. Kim SH, Chang KH, Song IC, et al. Brain abscess and brain tumor: discrimination with in vivo H-1 MR spectroscopy. Radiology 1997;204(1):239–45.
43. Pal D, Bhattacharyya A, Husain M, et al. In vivo proton MR spectroscopy evaluation of pyogenic brain abscesses: a report of 194 cases. AJNR Am J Neuroradiol 2010;31(2):360–6.
44. Bulik M, Jancalek R, Vanicek J, et al. Potential of MR spectroscopy for assessment of glioma grading. Clin Neurol Neurosurg 2013;115(2):146–53.
45. Wang Q, Zhang H, Zhang J, et al. The diagnostic performance of magnetic resonance spectroscopy in differentiating high-from low-grade gliomas: A systematic review and meta-analysis. Eur Radiol 2016;26(8):2670–84.
46. Siu A, Wind JJ, Iorgulescu JB, et al. Radiation necrosis following treatment of high grade glioma–a review of the literature and current understanding. Acta Neurochir (Wien) 2012;154(2):191–201 [discussion: 201].
47. Parvez K, Parvez A, Zadeh G. The diagnosis and treatment of pseudoprogression, radiation necrosis and brain tumor recurrence. Int J Mol Sci 2014;15(7):11832–46.
48. Brandes AA, Franceschi E, Tosoni A, et al. MGMT promoter methylation status can predict the incidence and outcome of pseudoprogression after concomitant radiochemotherapy in newly diagnosed glioblastoma patients. J Clin Oncol 2008;26(13):2192–7.
49. Wen PY, Macdonald DR, Reardon DA, et al. Updated response assessment criteria for high-grade gliomas: response assessment in neuro-oncology working group. J Clin Oncol 2010;28(11):1963–72.
50. Zhang H, Ma L, Wang Q, et al. Role of magnetic resonance spectroscopy for the differentiation of recurrent glioma from radiation necrosis: a systematic review and meta-analysis. Eur J Radiol 2014;83(12):2181–9.
51. Nakajima T, Kumabe T, Kanamori M, et al. Differential diagnosis between radiation necrosis and glioma progression using sequential proton magnetic resonance spectroscopy and methionine positron emission tomography. Neurol Med Chir (Tokyo) 2009;49(9):394–401.
52. van Dijken BRJ, van Laar PJ, Holtman GA, et al. Diagnostic accuracy of magnetic resonance imaging techniques for treatment response evaluation in patients with high-grade glioma, a systematic review and meta-analysis. Eur Radiol 2017;27(10):4129–44.
53. Zakhari N, Taccone MS, Torres C, et al. Diagnostic accuracy of centrally restricted diffusion in the differentiation of treatment-related necrosis from tumor recurrence in high-grade gliomas. AJNR Am J Neuroradiol 2018;39(2):260–4.
54. Nassirpour S, Chang P, Avdievitch N, et al. Compressed sensing for high-resolution nonlipid suppressed (1) H FID MRSI of the human brain at 9.4T. Magn Reson Med 2018;80(6):2311–25.
55. Strasser B, Povazan M, Hangel G, et al. (2 + 1)D-CAIPIRINHA accelerated MR spectroscopic imaging of the brain at 7T. Magn Reson Med 2017;78(2):429–40.
56. Thomas MA, Nagarajan R, Huda A, et al. Multidimensional MR spectroscopic imaging of prostate cancer in vivo. NMR Biomed 2014;27(1):53–66.
57. Ebel A, Soher BJ, Maudsley AA. Assessment of 3D proton MR echo-planar spectroscopic imaging

using automated spectral analysis. Magn Reson Med 2001;46(6):1072–8.
58. Ebel A, Maudsley AA. Improved spectral quality for 3D MR spectroscopic imaging using a high spatial resolution acquisition strategy. Magn Reson Imaging 2003;21(2):113–20.
59. Mansfield P. Spatial mapping of chemical shift in NMR. Magn Reson Med 1984;1:370–86.
60. Posse S, Cuenod CA, Risinger R, et al. Anomalous transverse relaxation in 1H spectroscopy in human brain at 4 Tesla. Magn Reson Med 1995;33(2):246–52.
61. Lin FH, Tsai SY, Otazo R, et al. Sensitivity-encoded (SENSE) proton echo-planar spectroscopic imaging (PEPSI) in the human brain. Magn Reson Med 2007;57(2):249–57.
62. Tsai SY, Otazo R, Posse S, et al. Accelerated proton echo planar spectroscopic imaging (PEPSI) using GRAPPA with a 32-channel phased-array coil. Magn Reson Med 2008;59(5):989–98.
63. Zhu X, Ebel A, Ji JX, et al. Spectral phase-corrected GRAPPA reconstruction of three-dimensional echo-planar spectroscopic imaging (3D-EPSI). Magn Reson Med 2007;57(5):815–20.
64. Ebel A, Maudsley AA. Comparison of methods for reduction of lipid contamination for in vivo proton MR spectroscopic imaging of the brain. Magn Reson Med 2001;46(4):706–12.
65. Nelson SJ, Li Y, Lupo JM, et al. Serial analysis of 3D H-1 MRSI for patients with newly diagnosed GBM treated with combination therapy that includes bevacizumab. J Neurooncol 2016;130(1):171–9.
66. Jin T, Ren Y, Zhang H, et al. Application of MRS- and ASL-guided navigation for biopsy of intracranial tumors. Acta Radiol 2019;60(3):374–81.
67. Scott JN, Brasher PM, Sevick RJ, et al. How often are nonenhancing supratentorial gliomas malignant? A population study. Neurology 2002;59(6):947–9.
68. Henson JW, Gaviani P, Gonzalez RG. MRI in treatment of adult gliomas. Lancet Oncol 2005;6(3):167–75.
69. Jacobs AH, Kracht LW, Gossmann A, et al. Imaging in neurooncology. NeuroRx 2005;2(2):333–47.
70. Weber MA, Giesel FL, Stieltjes B. MRI for identification of progression in brain tumors: from morphology to function. Expert Rev Neurother 2008;8(10):1507–25.
71. Cordova JS, Shu HK, Liang Z, et al. Whole-brain spectroscopic MRI biomarkers identify infiltrating margins in glioblastoma patients. Neuro Oncol 2016;18(8):1180–9.
72. Nelson SJ, Graves E, Pirzkall A, et al. In vivo molecular imaging for planning radiation therapy of gliomas: an application of 1H MRSI. J Magn Reson Imaging 2002;16(4):464–76.
73. Pirzkall A, McKnight TR, Graves EE, et al. MR-spectroscopy guided target delineation for high-grade gliomas. Int J Radiat Oncol Biol Phys 2001;50(4):915–28.
74. Ken S, Vieillevigne L, Franceries X, et al. Integration method of 3D MR spectroscopy into treatment planning system for glioblastoma IMRT dose painting with integrated simultaneous boost. Radiat Oncol 2013;8:1.
75. Cordova JS, Kandula S, Gurbani S, et al. Simulating the effect of spectroscopic MRI as a metric for radiation therapy planning in patients with glioblastoma. Tomography 2016;2(4):366–73.
76. Gurbani S, Weinberg B, Cooper L, et al. The brain imaging collaboration suite (BrICS): a cloud platform for integrating whole-brain spectroscopic MRI into the radiation therapy planning workflow. Tomography 2019;5(1):184–91.